A 28-GHz CMOS LNA with Stability-Enhanced G_m-Boosting Technique Using Transformers

Sunwoo Kong[1], Hui-Dong Lee, Seunghyun Jang, Jeehoon Park, Kwang-Seon Kim, Kwang-Chun Lee
ETRI (Electronics and Telecommunications Research Institute)
Gajeong-ro 218, Yuseong-gu, Daejeon, South Korea
[1]swkong@etri.re.kr

***Abstract* — In this paper, we propose a low noise amplifier (LNA) using a g_m-boosting technique with improved stability using transformers in the millimeter-wave (mm-Wave) band. The transformer composed of three inductors improves not only stability, but also gain and low-noise performance of the LNA. The conditions for stability shows that the proposed structure can guarantee good stability over a high frequency range. The chip was fabricated using the TSMC 65-nm CMOS process and it has an active chip area of 0.11 μm^2. The fabricated LNA has a gain of 18.33 dB and a noise figure (NF) of 3.25–4.2 dB. The stability factor μ values are 9.7 and 5.2 at the source and load sides of the LNA, respectively. The 3-dB bandwidth of the LNA is 24.9–32.5 GHz and the chip consumes 17.1-mA current from a 1.2-V supply.**

***Keywords* — LNA, transformer, gm-boosting, stability**

I. Introduction

The bandwidth of the wireless communication system is gradually increasing with the demand of high data rates. Recently, in order to guarantee a wide bandwidth, the operation frequency has started to expand to the millimeter-wave (mm-Wave) band, and 5G cellular network is one of the promising mm-Wave application. A low noise amplifier (LNA) is a component that greatly affects the sensitivity of the system depending on its performance. The performance such as noise figure (NF), gain, bandwidth, and power consumption of the LNA are in a trade-off relationship with each other. In mm-Wave frequency, the stability problem is likely to occur and the performance degradation due to the signal loss is remarkable because the influence of the parasitic component increases. The cascode structure is one of good candidates for improving performance while ensuring stability. The cascode structure can increase the gain and reduce power consumption by stacking common-source (CS) stage and common-gate (CG) stage. Since the cascode structure has high input to output isolation, it ensures good stability.

However, in the mm-Wave band, the influence of the parasitic cap C_{p1} which is at the connection point of the CS and CG satges increases and the signal leaks through it as shown in Fig. 1a. To solve this problem, the inductors connected in series and in parallel are used to compensate for the effect of C_{p1} and C_{p2}, in Fig. 1b and 1c [1][2]. Furthermore, Fig. 1d shows a structure that improves gain and NF of the amplifier while compensating C_{p1} and C_{p2} using a transformer which is composed of L_{SG} and L_P [3]. This structure boosts effective g_m of the CG stage by constructing a negative feedback network using the transformer, so the conditions for negative feedback must be maintained. Moreover, the cascode with a transformer poses a potential risk of the stability problem due to the inductor connected to the gate of the CG stage [4].

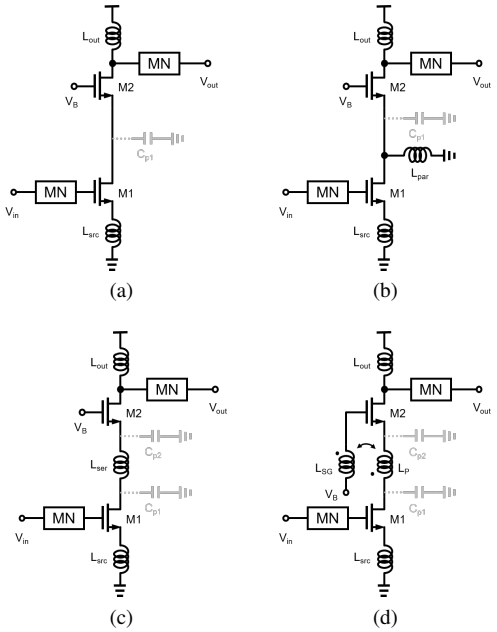

Fig. 1. Stacked LNAs. (a) Cascode. (b) Cascode with a parallel inductor. (c) Cascode with a series inductor. (d) Cascode with a transformer.

We have proposed an LNA using a g_m-boosting technique with improved stability using transformers in the mm-Wave band. The stability problem of the g_m-boosting technique using transformers was analyzed and new transformers were designed to solve it.

II. Circuit Design

A. Stability-Enhanced G_m-Boosting Technique

Fig. 2a shows a cascode LNA with the proposed stability-enhanced g_m-boosting technique. Transistors M_1 and M_2 constitute CS and CG structures, respectively. Transformers consisting of three inductors, which are L_P, L_{SG}, and L_{SD}, are placed around M_2. L_P is located between the source of M_2 and the drain of M_1, and L_{SG} is connected to the gate of M_2. To enlarge gate-source voltage swing for g_m-boosting, anti-phase relationship due to the magnetic coupling between L_P and L_{SG} is used. L_{SD} is connected to the drain of M_2. The effect of gate-drain capacitance is

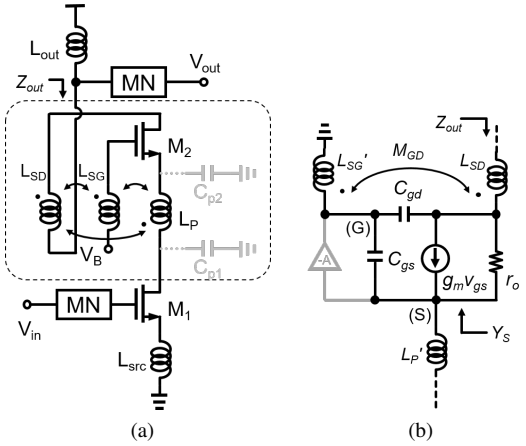

Fig. 2. (a) Schematic of the proposed LNA with transformers consisting of L_P, L_{SG}, and L_{SD}. (b) Simplified equivalent model of the circuit in the dotted box around M_2 in Fig. 2a.

neutralized using the magnetic coupling between L_{SD} and L_{SG} and they make in-phase relationship at the drain and gate of M_2. The transformer composed of L_P and L_{SG} cancels the effects of C_{p1} and C_{p2} and can be represented by L'_P and L'_{SG} in Fig. 2b [3]. L'_{SG} and C_{gs} form a negative feedback factor of A between source and gate. Fig. 2b shows a simplified equivalent model of the circuit in the dotted box around M_2 in Fig. 2a. Without L_{SD}, feedback factor A can be expressed as

$$A = \frac{j\omega L'_{SG}}{1/\omega C_{gs} - \omega L'_{SG}} \tag{1}$$

where C_{gs} is the gate-to-source capacitance of M_2. To maintain negative feedback, $\omega < 1/\sqrt{L'_{SG}C_{gs}}$ must be met. Applying the mutual inductance M_{GD} of the transformer formed by L_{SD} and L'_{SG}, feedback factor becomes

$$A' = \frac{j\omega C_{gs}(j\omega L'_{SG} + \omega_t M_{GD})}{1 + j\omega C_{gs}(j\omega L'_{SG} + \omega_t M_{GD})} \tag{2}$$

where $\omega_t = g_m/C_{gs}$ and g_m are the angular cutoff frequency and trans-conductance of M_2, respectively. The effective g_m of M_2 is boosted as

$$G_m = (1 + A')g_m. \tag{3}$$

Y_S is the admittance seen in (S) and the conductance part is expressed as

$$Re(Y_S) = \frac{(1 - \omega^2(L'_{SG} - M_{GD})C_{gs})g_m}{(1 - \omega^2 L'_{SG}C_{gs})^2 + (\omega M_{GD}g_m)^2}. \tag{4}$$

If $M_{GD} > L'_{SG}$, the proposed structure is stable because $Re(Y_S)$ is always positive. If $M_{GD} < L'_{SG}$, the proposed structure is stable when the following condition is maintained:

$$\omega < \frac{1}{\sqrt{(L'_{SG} - M_{GD})C_{gs}}}. \tag{5}$$

When a transformer composed of L_{SD} and L'_{SG} is applied, the proposed g_m-boosted topology has always stable condition or a wider stable band than when it is not.

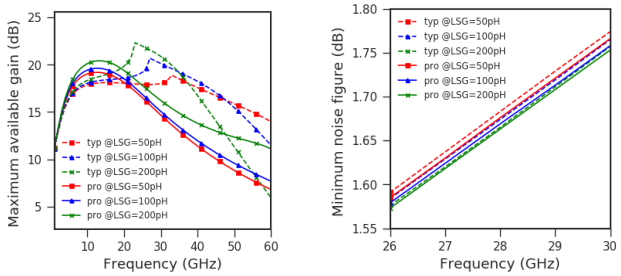

Fig. 3. Simulated (a) MAGs and (b) NFs of the proposed structure (Fig. 1d) and the typical cascode structure with a transformer (Fig. 2a) when L_{SG}s are 50 pH, 100 pH, and 200 pH.

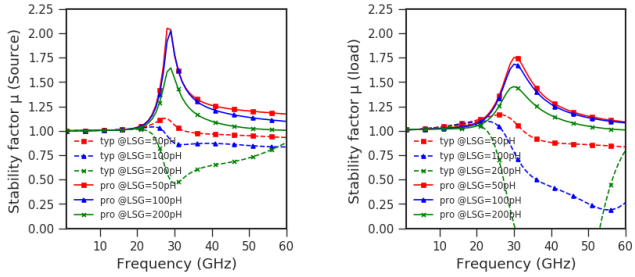

Fig. 4. Simulated stability factors (a) μ (source) and (b) μ (load) of the proposed structure (Fig. 1d) and the typical cascode structure with a transformer (Fig. 2a) when L_{SG}s are 50 pH, 100 pH, and 200 pH.

Fig. 3a shows that the simulated maximum available gain (MAG)s of the proposed structure (Fig. 2a) and the typical cascode structure with a transformer (Fig. 1d) increase as the value of L_{SG} increases. The two structures commonly have transistor size of 36 μm and coupling factor k of 0.7 for L_P (100 pH) and variable L_{SG}s (50 pH, 100 pH, and 200 pH). For the proposed structure, L_{SD} has a value of 100 pH and the coupling factors between L_{SG} and L_{SD} and between L_P and L_{SD} are 0.7 and 0.6, respectively. Fig. 4a and Fig. 4b show the stability factors (μ) of load and source. The magnitude of μ is a measure of the stability and the larger value of the μ, the higher the stability of 2-port systems. Due to the coupling between L_{SD} and L_{SG}, the proposed structure is stable in all bands with all L_{SG} values. However, the upper band of the stable region of the typical structure decreases as the gate inductor value increases. The minimum NF is shown in Fig. 3b and there is slight NF improvement with the stability-enhanced G_m-boosting technique.

The impedance seen at the output node in Fig. 2b, Z_{out}, is shown on a Smith chart for three types of circuit configurations (OA, OB, and OC) in Fig. 5.

- OA: typical cascode with transformer (without L_{SD})
- OB: typical cascode with transformer (with L_{SD})
- OC: proposed structure (with L_{SD} and M_{GD})

For the three configurations, Z_{out}s are displayed when the values of the gate inductors are varied from 50 pH to 200 pH. In the configuration OA and OB, increasing the value of

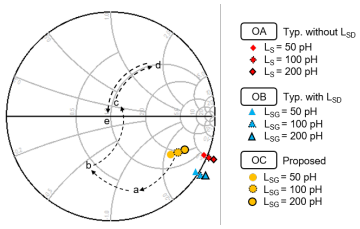

Fig. 5. Output impedance transformation on Smith Chart with different gate inductors. Z_{out} starts from three different points OA, OB, and OC.

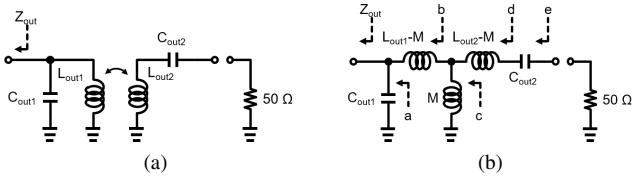

Fig. 6. Simplified output matching circuit: (a) output transformer and (b) its equivalent circuit.

L_{SG} causes the amplifier to go into the unstable region. Z_{out} is moved from OA to OB by adding L_{SD}. L_{SD} provides positive reactance term to Z_{out}. Z_{out} shifts from OA to OC as the real impedance and reactance are added by the gate-drain transformer. In this case, stability is guaranteed against the change of L_{SG}. The transformer in Fig. 6a can be used to match Z_{out} to 50 ohms. The transformer performs the function of matching and differential to single ended conversion. Fig. 5 shows the transformed trace of Z_{out} from a to e adding the matching components as an equivalent model of the transformer in Fig. 6b.

B. Circuit Implementation

Fig. 7 shows the overall differential schematic of the proposed LNA. Section II-A explained the single-ended structure of the proposed LNA. In this section, the proposed technique is applied to the differential structure which is robust to noise and effects of bond wires and system integration issues are also considered. The first and second stage uses a CS and cascode structure, respectively, and the source degeneration inductors L_{src1} and L_{src2} are used for input matching. The input matching circuit is composed of a single-ended to differential transformer and the output stage uses a differential to single-ended transformer. The first and the second stages are matched by an inter-stage transformer. The CS stage compensates the gate-to-drain feedback cap using a drain-to-gate transformer [5]. The cascode stage uses the proposed stability-enhanced g_m-boosting technique.

III. Measurement

The chip was fabricated using TSMC 65-nm CMOS process. Fig. 8 shows a micrograph of the fabricated chip. The chip size is 750 x 500 μm^2 including pads and the active chip area is 490 x 230 μm^2. The performance of the fabricated LNA was investigated by on-probe measurement. At a supply voltage of 1.2 V, 17.1-mA current was consumed. Fig. 9 compares the measured S-parameter of the fabricated

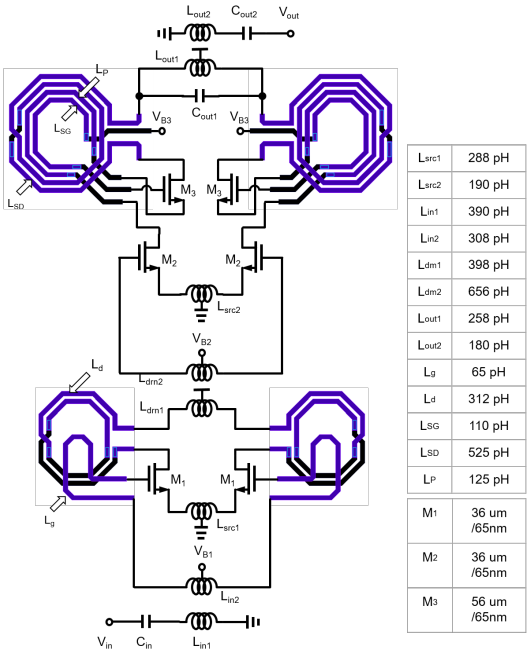

L_{src1}	288 pH
L_{src2}	190 pH
L_{in1}	390 pH
L_{in2}	308 pH
L_{drn1}	398 pH
L_{drn2}	656 pH
L_{out1}	258 pH
L_{out2}	180 pH
L_g	65 pH
L_d	312 pH
L_{SG}	110 pH
L_{SD}	525 pH
L_P	125 pH
M_1	36 um /65nm
M_2	36 um /65nm
M_3	56 um /65nm

Fig. 7. Schematic of the proposed differential LNA

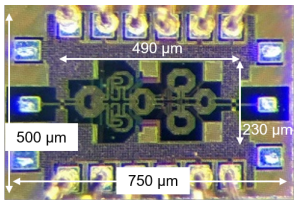

Fig. 8. Micrograph of the chip.

LNA with the simulated S-parameter of it. The measured gain is 18.33 dB and the simulation gain is 21.8 dB at 28 GHz. The 3-dB bandwidth for measurement and simulation are 7.6 GHz (24.9–32.5 GHz) and 5.6 GHz (25.6–31.2 GHz), respectively. The measurement results has lower peak S21 and wider bandwidth than the simulation results because the measured S22 is down-shifted from the simulation result. Fig. 10 compares the measured NF with the simulation results. The both of NFs have similar values because S11 was matched. The measured NF is 3.25 dB at 28 GHz. An Agilent PNA-X N5247B instrument was used for cold-source NF measurements and the wideband power sensor was the Agilent U2011XA instrument. As shown in Fig. 11, the stability factor μ has values of 9.7 and 5.2 on the source and load sides. The peak value of μ is 27 and 20 for the source and load. the fabricated LNA is unconditionally stable because $\mu > 1$ over the entire 20–40 GHz band.

Table 1 summarizes the performance of the proposed LNA and compares it with state of the art results. The LNA has the lowest NF and the smallest active chip area with full differential structure. Also, the gain per power consumption of this work is the second highest in the comparison group. The LNA has a higher stability factor μ than the other work

Table 1. Performance summary and comparison with state of the art

	This work	**[6]**	**[2]**	**[7]**
Freq [GHz]	24.9–32.5	26–33	33‡	16–30
Tech.	65 nm	40 nm	28 nm	65 nm
Stages	1 Diff. CS, 1 Diff. Cas.	1 Cas., 2 Diff. CS	2 Cas.	1 Cas.
Gain [dB]	18.33	27.1/18.4	18.6	10.2
NF [dB]	3.25-4.2	3.3-4.4	4.9	3.3-5.7
S12 [dB]	-47	-38†	-45	-
μ (source, load)	9.7, 5.2	-	3, 5†	-
P1dB [dBm]	-24	-21.6/-13.4	-25.5	N/A
Power [mW]	20.5 @1.2 V	31.4/21.5 @1.1 V	9.7 @1.2 V	12.4 @N/A
Act./total area [mm^2]	0.11/0.38	0.26/0.54†	0.23/0.51†	0.13†/0.18

† Graphically estimated. ‡ 3-dB Bandwidth of 4.7 GHz.

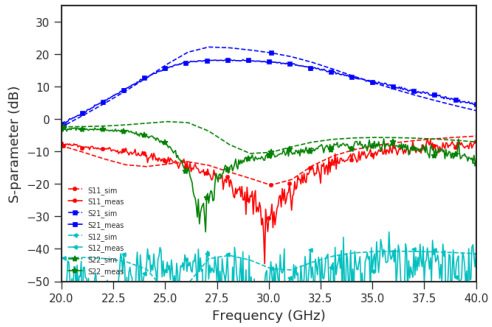

Fig. 9. Comparison of measured and simulated S-parameters of the LNA.

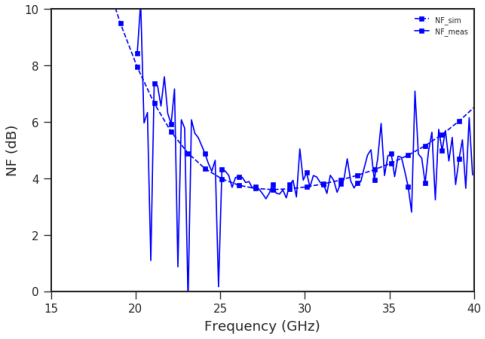

Fig. 10. Comparison of measured and simulated NF of the LNA.

which reported stability factors. It was also confirmed that the LNA had the lowest reverse isolation S12, which is an indirect indicator for good stability.

IV. Conclusion

In this paper, we proposed an LNA using a stability-enhanced g_m-boosting technique with transformers consisting of three inductors in the mm-Wave band. The g_m-boosting technique brought the LNA good gain and low-noise results per power consumption. The comparison of the conditions for stability shows that the proposed structure can guarantee good stability over a wider frequency range. The fabricated LNA has the stability factor μ values of 9.7 and 5.2 at the source and load sides, respectively, and 3.25–4.2-dB NF with 18.33-dB gain at the same time.

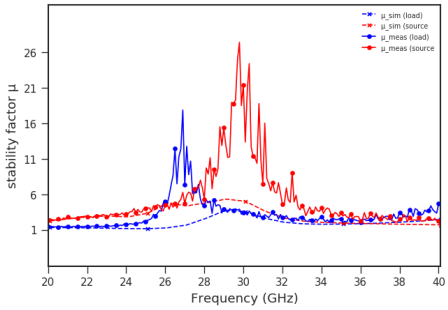

Fig. 11. Comparison of measured and simulated stability factor μ of the LNA.

Acknowledgment

This work was supported by Institute for Information & communications Technology Promotion (IITP) grant funded by the Korea government (MSIT) (No. 2017-0-00409, Development on millimeter-wave beamforming IC for 5G mobile communication).

References

[1] H. Samavati, H. R. Rategh, and T. H. Lee, "A 5-GHz CMOS Wireless LAN Receiver Front End," *IEEE J. Solid-State Circuits*, vol. 35, no. 5, pp. 765–772, 2000.

[2] M. K. Hedayati, A. Abdipour, R. S. Shirazi, C. Cetintepe, and R. B. Staszewski, "A 33-GHz LNA for 5G Wireless Systems in 28-nm Bulk CMOS," *IEEE Trans. Circuits Syst. II Express Briefs*, vol. 65, no. 10, pp. 1460–1464, 2018.

[3] S. Guo, T. Xi, P. Gui, D. Huang, Y. Fan, and M. Morgan, "A Transformer Feedback Gm-Boosting Technique for Gain Improvement and Noise Reduction in mm-Wave Cascode LNAs," *IEEE Trans. Microw. Theory Tech.*, vol. 64, no. 7, pp. 2080–2090, 2016.

[4] Hsieh-Hung Hsieh and Liang-Hung Lu, "A 40-GHz Low-Noise Amplifier With a Positive-Feedback Network in 0.18-um CMOS," *IEEE Trans. Microw. Theory Tech.*, vol. 57, no. 8, pp. 1895–1902, 2009.

[5] M. P. van der Heijden, L. C. N. de Vreede, and J. N. Burghartz, "On the Design of Unilateral Dual-Loop Feedback Low-Noise Amplifiers With Simultaneous Noise, Impedance, and IIP3 Match," *IEEE J. Solid-State Circuits*, vol. 39, no. 10, pp. 1727–1736, 2004.

[6] M. Elkholy, S. Shakib, J. Dunworth, V. Aparin, and K. Entesari, "A Wideband Variable Gain LNA With High OIP3 for 5G Using 40-nm Bulk CMOS," *IEEE Microw. Wirel. Components Lett.*, vol. 28, no. 1, pp. 64–66, 2018.

[7] P. Qin and Q. Xue, "Compact Wideband LNA With Gain and Input Matching Bandwidth Extensions by Transformer," *IEEE Microw. Wirel. Components Lett.*, vol. 27, no. 7, pp. 657–659, 2017.